Ultrafast electron dynamics at metal surfaces: Competition between electron-phonon coupling and hot-electron transport

Mischa Bonn,* Daniel N. Denzler, Stephan Funk, and Martin Wolf
Fritz Haber Institut der Max-Planck Gesellschaft, Faradayweg 4-6, D-14195 Berlin, Germany

S.-Svante Wellershoff and Julius Hohlfeld
Fachbereich Physik, Freie Universität Berlin, Arnimallee 14, D-14195 Berlin, Germany
(Received 28 June 1999)

An experimental scheme (double pump/reflectivity probe using femtosecond laser pulses) enables the investigation of nonequilibrium electron dynamics at metal surfaces by measuring the equilibrated surface temperature. The competition between electron-phonon coupling and hot-electron transport gives rise to a reduced equilibrated temperature when the two pump pulses overlap in time, and provides a way of accurately determining the electron-phonon coupling constant. These observations have important consequences for femtosecond photochemical investigations.

INTRODUCTION

A deeper understanding of ultrafast dynamics of electrons in metals is essential from both a fundamental and a technological point of view. Electron and phonon dynamics following short-pulse optical excitation of the metal electrons govern, for instance, photochemical processes such as photoinduced surface reactions (e.g., photodesorption[1]) and laser ablation.[2,3] Electron dynamics have therefore been intensely investigated using femtosecond laser spectroscopy.[4–12] In these experiments, an ultrashort excitation (''pump'') pulse heats the electrons at the metal surface. Rapid thermalization within the electron gas to a Fermi–Dirac distribution — which has been observed with time-resolved photoemission spectroscopy[10] — occurs by electron-electron scattering. Due to the relatively small electronic heat capacity, peak electronic temperatures of thousands of K above the equilibrium melting point can be reached. Ballistic transport of nonthermalized electrons[7,8] and diffusive transport of thermalized electrons into the bulk takes place, while simultaneously heat is transferred from the electronic system to the initially cold lattice by electron-phonon coupling. The rate of electron-phonon heat transfer is determined by the electron-phonon coupling constant, a key parameter in superconductivity theory.[12,13] The electron dynamics can be followed by probing the transient optical reflectivity changes with a second (''probe'') pulse. However, as pointed out by Groeneveld *et al.*[11] and Brorson *et al.*,[12] the weakness of this technique lies in the difficulty of relating the observed reflectivity changes ΔR to changes in the electron and phonon temperatures T_e and T_l at a given probe frequency ω: $\Delta R(T_e,T_l,\omega)$. This is illustrated in Fig. 1, which depicts ΔR of gold at two slightly different wavelengths upon excitation with two pump pulses.

It is the purpose of this paper to demonstrate that it is possible to obtain information on femtosecond *nonequilibrium* electron dynamics following optical excitation by measuring an *equilibrium* quantity: the reflectivity of the equilibrated surface. This is accomplished by using two pump pulses instead of one, and monitoring the surface reflectivity as a function of delay between the pump pair, sufficiently long after the pump pair to ensure complete electron-phonon thermalization. Thus, we circumvent the major drawback of the one-pulse excitation experiments, the difficulty in relating the observed ΔR to changes in T_e and T_l. This is of special relevance for systems with complicated electronic structures like transition metals and superconductors:[6] The reflectivity changes measured with the technique presented here can be directly related to temperature by a simple calibration measurement.

EXPERIMENT

The experiments were performed with a commercial (Coherent) laser system delivering 400 nm (pump) as well as

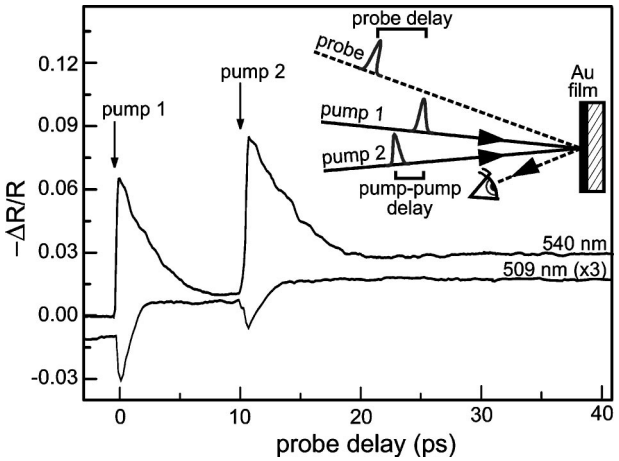

FIG. 1. Measured reflectivity changes (corresponding to electronic temperature rises of ~1000 K) for a 700 nm gold film caused by excitation pulses centered at $t=0$ and $t=10.5$ ps for two wavelengths. The inset shows the experimental pump-pump-probe setup. The different relaxation times (under identical excitation conditions) illustrate the necessity of knowing $R(T_e,T_l,\omega)$ to interpret this type of experiment. Data are offset for clarity.

tunable (probe) pulses of 200 fs duration at a 15 kHz repetition rate. Pump-induced reflection changes (noise level $\sim 5 \times 10^{-5}$) are detected using lock-in techniques. The *p*-polarized probe and two equally strong *s*-polarized pump pulses are focused onto the metal surface (normal incidence) by the same 30 mm lens. The focus of the ~ 40 μm probe beam is approximately eight times smaller than the pump foci, to ensure radially homogeneous excitation over the probed surface. All experiments were performed in air at room temperature on commercial polycrystalline gold and chromium films of variable thickness (on quartz substrates), as well as on freshly polished copper [100] and ruthenium [001] single crystals. The typical fluence of one excitation pulse was about 20 $\mathrm{J\,m^{-2}}$, creating transient electronic and lattice temperature increases in gold of ~ 1000 K and ~ 30 K, respectively. The probe photon energies were chosen to maximize reflectivity changes with temperature.

RESULTS AND DISCUSSION

A. Electron dynamics in gold

Figure 1 depicts the transient change in surface reflectivity of a 700 nm gold film, upon excitation with two pump pulses. The experimental scheme is shown in the inset. In the experiment depicted in this figure, the probe delay is scanned with the pump-pump delay fixed at 10.5 ps. The different relaxation times at different probe wavelengths demonstrate that to extract information on, e.g., the electron-phonon coupling strength from this experiment, it is necessary to have full knowledge of $R(T_e, T_l, \omega)$. To avoid this problem we focus in this paper on experiments in which the pump-pump delay is scanned, whereas the probe delay is fixed at a sufficiently high value to ensure complete thermalization between electrons and phonons. Results for scanning the pump-pump delay with the probe delay set at 250 ps after the fixed pump pulse are depicted in the upper panel of Fig. 2 for gold films of varying thickness. The slight asymmetry (higher signal for positive delays) is due to the fact that the probe delay is set with respect to the temporally fixed pump pulse. Strikingly, for the thicker films (thickness $\geqslant 300$ nm), a dip in reflectivity of $\sim 6\%$ in the total signal is observed at zero pump-pump delay. It corresponds to a *decrease* in equilibrium surface temperature, when the two excitation pulses irradiate the surface simultaneously compared to the case when the two excitation pulses are slightly separated in time. This somewhat counterintuitive result—a *lower* final surface temperature after excitation with a *higher* power density—is absent for thin films (thickness $\leqslant 200$ nm). Since all films are optically equivalent (significantly thicker than the ~ 16 nm optical penetration depth,[14]) the dip cannot be caused by an optical artifact such as bleaching. This is further corroborated by a simple pump-probe experiment, which shows no reflectivity change ($\Delta R/R \leqslant 10^{-3}$) when both wavelengths are set to 400 nm. The dip could in principle be caused by an electron temperature (and hence power density) dependence of the electron-phonon coupling strength, as suggested previously.[15] However, a thorough investigation unequivocally demonstrates that there is no fluence dependence of the electron-phonon coupling strength for gold, for power densities up to the damage threshold.[16] The dip also disappears with increasing delay between the pump pair and the probe pulse for constant film thickness (700 nm), as demonstrated in the lower panel of Fig. 2.

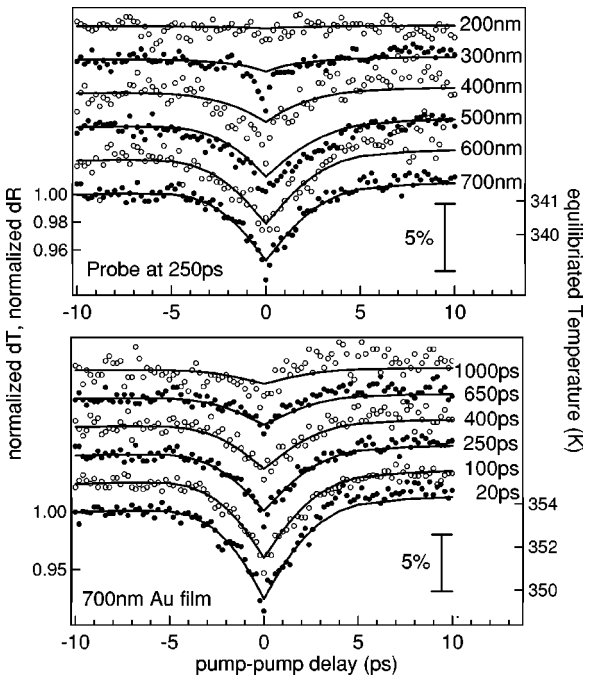

FIG. 2. Measured reflectivity changes as a function of the pump-pump delay. Upper panel: gold films of varying thickness, at fixed probe delay (250 ps after the temporally fixed pump pulse). Lower panel: fixed film thickness (700 nm) for several probe delay times. A dip in reflectivity, corresponding to a decrease in surface temperature, is observed when the two excitation pulses overlap temporally. The experimentally observed reflectivity changes (dots) and the calculated temperatures (lines) are normalized to the average value between $-10 \leqslant \tau \leqslant -5$ ps. For the bottom curve in each graph, absolute temperatures are indicated. Data are offset for clarity.

From Fig. 1 it is apparent that the electron-phonon thermalization is over after ~ 10 ps. Therefore, for the probe delays in Fig. 2 ($\geqslant 20$ ps), complete thermalization between electrons and phonons has occurred. The dip observed at these long delay times reflects the short-time dynamics taking place as the two pumps overlap in time. *This means that we obtain information about ultrafast femtosecond electron dynamics by looking — much later — at a thermalized system.* This makes this technique an important tool in the investigation of electron dynamics.

B. Theoretical description

To understand the origin of the dip, we have modeled our data by means of the two-temperature model.[17] In this model, the electron and phonon subsystems are described by two separate heat baths with temperatures T_e and T_l. For the high fluences (~ 10 $\mathrm{J\,m^{-2}}$) used in the experiments, it has been demonstrated that electron thermalization in gold is fast compared to the 200 fs duration of our pulses,[9–11] justifying the use of an electronic temperature. Treatment of the problem can be reduced to one spatial dimension (the *z* axis perpendicular to the surface), as (i) the (radial) temperature gradient in the probed surface area is negligible (probe diameter being much less than pump diameter) compared to the gra-

dient along the z axis and (ii) the radial heat diffusion length is much smaller than the pump diameter even after 1000 ps (the longest probe delay used). Therefore the expressions for the time evolution of the temperatures read

$$C_e(T_e)\frac{\partial T_e}{\partial t}=\frac{\partial}{\partial z}\left(\kappa\frac{\partial}{\partial z}T_e\right)-g(T_e-T_l)+S(z,t),$$

$$C_l(T_l)\frac{\partial T_l}{\partial t}=g(T_e-T_l).$$

C_e and C_l are the electronic and phonon heat capacities, respectively. In our simulations C_l is calculated within the Debye approximation.[18] The first equation describes (i) electron diffusion (κ is the electron thermal conductivity), (ii) electron-phonon coupling (coupling strength g), and (iii) heating of the electrons by the laser pulse [the source term $S(z,t)$ is the absorbed laser energy density per unit time]. The diffusive term is absent in the second equation, because heat diffusion occurs much more rapidly through the electron gas than through the lattice phonons. The effect of ballistic electron transport — the electron mean free path in gold has been determined to be $\sim$100 nm in these films at room temperature[7] — is incorporated in the calculations by increasing the optical penetration depth by 100 nm.[19] This approach is valid because the ballistic transport is fast (100 nm in 100 fs) compared to the pulse duration.

The final surface temperature is determined by a competition between electron-phonon coupling and hot electron diffusion. Electron-phonon coupling will tend to localize the heat at the surface, whereas hot electron diffusion will result in heat transport away from the surface, into the bulk. The dynamics of the electron heating and cooling process is nonlinear since there is a temperature dependence for the electron specific heat ($C_e=\gamma T_e$), as well as for the electron thermal conductivity ($\kappa=\kappa_0[T_e/T_l]$ for temperatures below a critical temperature,[20] $\sim$4000 K for gold; even higher for the other metals discussed here). It is the resulting nonlinearity in $(\partial/\partial z)[\kappa(\partial/\partial z)T_e]$ with respect to T_e that gives rise to the observed dip in the final (electron and phonon) surface temperature: When the two excitation pulses overlap in time, the thermal conduction will be large due to the high transient electronic temperature, so that strong diffusive transport of the hot electrons away from the surface will take place, effectively cooling the surface. If the pulses are temporally separated, the peak electronic temperature, and therefore the heat conduction, is reduced, so that the surface cools relatively slowly. In other words, the effective electron diffusion length depends on the delay between the two excitation pulses. This is illustrated in Fig. 3, which depicts calculated spatial temperature profiles of a 700 nm gold film for different pump-pump delays. Clearly, for shorter pump-pump delays the heat has penetrated deeper into the film, caused by a larger effective electron diffusion length, so that the surface is cooler compared to longer delays. This results in the surface temperature dip shown in the inset. Of course, after a certain time the gold film will be homogeneously heated, which explains the disappearance of the dip with ''waiting time'' (probe delay), as shown in the lower panel of Fig. 2. For thinner films, homogeneous heating of the film will occur at earlier times, accounting for the disappearance of the dip as can be observed in the upper panel of Fig. 2.

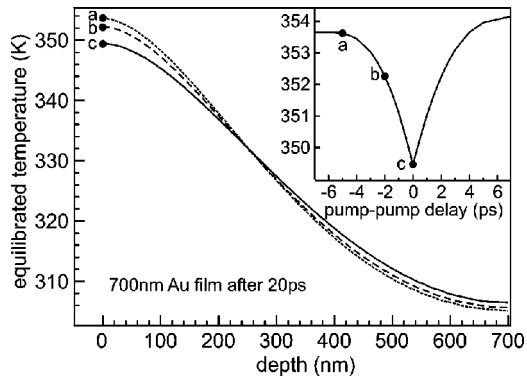

FIG. 3. Calculated spatial temperature profile of a 700 nm Au film 20 ps after the fixed pump pulse for three different pump-pump delays ($-5,-2,$ 0 ps marked by a, b, c, respectively; the trace in the inset is identical to the lowermost in Fig. 2). Note that, despite the fact that half of the energy is deposited earlier in case a compared to case c, the resulting surface temperature is higher (for case a the pulses are temporally located at -25 ps and -20 ps; for case c both pulses at -20 ps).

The coupled differential equations are solved by three different numerical schemes (fully explicit, fully implicit, and Crank-Nicholson[21]) that give identical results. Typical discretization dimensions in time and space are $dt=2\times10^{-17}$ s and $dx=1\times10^{-9}$ m (chosen to ensure numerical stability for given material parameters). Boundary conditions for the calculation are such that no heat transport occurs at the sample/air interface; for the films heat conduction to the substrate is negligible on picosecond timescales; bulk metal is treated as infinitely thick by expanding the spatial array when the last slab experiences a temperature increase exceeding 10^{-3} K. The material parameters used in the calculations are summarized in Table I.

As can be observed in Fig. 2, the simple model reproduces the experimental observations remarkably well: Although the depth of the dip is slightly underestimated, the shape of the dip is well accounted for. It was verified experimentally that ΔR is linearly proportional to changes in the surface temperature, as would be expected for these very small temperature variations ($\sim$3 K). It should be stressed that there are no free (''fit'') parameters in our calculation and no scaling factors were used.

C. Electron dynamics in other metals

Figure 4 depicts the dip for the metals copper, chromium, and ruthenium in comparison to gold. As can be observed, the dip becomes narrower with increasing electron-phonon coupling strength (see Table I). Again, the data are well described by the two-temperature model, demonstrating that this technique allows to investigate electron-phonon coupling dynamics in metallic systems in general: The width of the dip is limited by the electron-phonon equilibration time. Due to the extreme sensitivity of the dip shape to the exact value of the electron-phonon coupling strength, this important parameter can be accurately extracted. For the materials investigated, the observed dips can well be accounted for

TABLE I. Parameter values used in two-temperature model calculations.

Parameter		Au	Cu	Cr	Ru	
Electron-phonon coupling constant[a]	g	2.3	10	42	185	10^{16} W m^{-3} K^{-1}
Electron specific heat constant[b]	γ	71	98	194	400	J m^{-3} K^{-2}
Thermal conductivity (300 K)[b]	κ_0	317	401	94	117	W m^{-1} K^{-1}
Debye temperature[b]	θ	165	343	630	600	K
Atomic density[b]	n	5.9	8.5	8.3	7.4	10^{28} m^{-3}
Ballistic electron mean free path[c]	δ_{ball}	100	100	0	0	10^{-9} m
Optical penetration depth (400 nm)[d]	δ_{400}	16.3	14.4	8.9	6.9	10^{-9} m
Reflectivity (400 nm, incidence $<5°$)[d]	R_{400}	39.1	51.0	68.6	71.0	%

[a]Au, Refs. 12 and 19; Cu, Ref. 4 (see text); Cr, Ref. 12; Ru, Ref. 23 (see text).
[b]Reference 18.
[c]See explanation in text.
[d]Au, Ref. 14; Cu, Ref. 14; Cr, Ref. 14; Ru, Ref. 30.

with electron-phonon coupling constants from literature (see references in Table I). In the case of copper, where several experimental values differing by a factor of 10 have been reported,[2,4,12] our determination of $g=1\times10^{17}$ W m^{-3} K^{-1} supports the findings of Elsayed-Ali *et al.*[4,22] With the previously reported smaller values[2,12] of $g=1$ and 4.7×10^{16} W m^{-3} K^{-1} our experimental data cannot be reproduced. For ruthenium the value obtained here ($g=1.85\times10^{18}$ W m^{-3} K^{-1}) presents, to the best of our knowledge, the first experimental verification of the value obtained from theory.[23,24]

D. Consequences for photochemistry

Our findings have important consequences for photochemical experiments on adsorbate-covered metal surfaces with femtosecond pulses.[1,25–27] In these investigations, the key question is the photochemical reaction mechanism: The photochemical process can be induced either by coupling of the adsorbate to the hot electrons, or by coupling to the lattice phonons.[27] The generally employed experiment to investigate the coupling mechanism is a two-pulse correlation measurement,[25] in which the photoreaction (desorption) yield is measured as a function of delay between two pulses of equal intensity. Our results demonstrate that the two-pulse correlation technique provides a unique way of discerning between electron- and phonon-mediated chemistry: If the photochemistry proceeds primarily by coupling to the phonons, a strong decrease (''dip'') in the yield should be observed at zero pump-pump delay, a consequence of the dip in phonon temperature. Using the standard friction model[28,29] to quantify this effect, we calculate that the photoyield of CO desorbing from Cu[100] (Ref. 26) decreases by $\sim$21% at zero delay for the experimental circumstances and coupling rates reported in that study.[26] The dip is more pronounced in the calculated desorption yield compared to the phonon temperature (a 21% as opposed to a 3.5% decrease around zero delay) due to the Arrhenius-type desorption dynamics, where the temperature enters the exponent. In the experiment,[26] however, the dip was not observed. Possible reasons for this discrepancy are firstly that the reported coupling parameters[26] are (partly) incorrect: From these experiments it was inferred that desorption occurs by coupling to both the electrons and the phonons, with different coupling strengths. The absence of the dip in the experimental data implies that the role of electrons in the desorption process was underestimated. A second possible explanation is that the friction model does not provide an adequate description of the desorption process for this system: The model employs equilibrium concepts such as an effective adsorbate temperature and Arrhenius-type desorption kinetics, whereas a full description would have to include nonequilibrium effects.

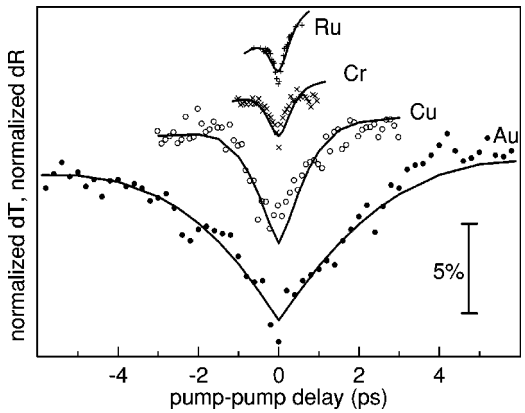

FIG. 4. Reflectivity changes for fixed probe delay times as a function of pump-pump delay for Au (700 nm film; the trace is identical to the lowermost in Fig. 2), Cu (bulk [100] crystal), Cr (200-nm film) and Ru (bulk [001] crystal). Lines are results of simulations described in the text; data are offset for clarity. Probe wavelengths are 490, 565, 660, and 606 nm, respectively, and probe delays 20, 15, 50, 15 ps. For Cu, the optical penetration depth is increased by 100 nm to account for ballistic electron transport, in analogy to Au; for Cr and Ru, ballistic effects are neglected, as electron thermalization occurs more rapidly.

CONCLUSION

Summarizing, we have developed and applied an experimental double pump/reflectivity probe scheme to investigate energy dynamics in metals. A dip in the equilibrated surface temperature is observed, if two excitation pulses excite the metal simultaneously. This can be explained by a competition between electron-phonon coupling and diffusive hot-

electron transport, and has important implications for surface photochemistry. By measuring equilibrated temperatures, the interpretation of this type of pump-probe experiments is greatly simplified compared to the conventional pump-probe technique. This may be of great importance to the study of electron dynamics of transition metals and other materials with complex electronic structures like high-T_c superconductors.

ACKNOWLEDGMENTS

We gratefully acknowledge Professor G. Ertl and Professor E. Matthias for continuous support and helpful discussions. This work was supported by the Deutsche Forschungsgemeinschaft, SFB 290. M.B. acknowledges financial support from the European Union (TMR Contract No. ERBFMBICT982971).

*Electronic address: bonn@fhi-berlin.mpg.de

[1] *Laser Spectroscopy and Photochemistry on Metal Surfaces*, edited by H.-L. Dai and W. Ho (World Scientific, Singapore, 1995), p. 625.

[2] P.B. Corkum, F. Brunel, N.K. Sherman, and T. Srinivasan-Rao, Phys. Rev. Lett. **61**, 2886 (1988).

[3] S.-S. Wellershoff, J. Güdde, J. Hohlfeld, J.G. Müller, and E. Matthias, Proc. SPIE **3343**, 378 (1998).

[4] H.E. Elsayed-Ali, T.B. Norris, M.A. Pessot, and G.A. Mourou, Phys. Rev. Lett. **58**, 1212 (1987).

[5] R.W. Schoenlein, W.Z. Lin, J.G. Fujimoto, and G.L. Eesley, Phys. Rev. Lett. **58**, 1680 (1987); N. Del Fatti, R. Bouffanais, F. Vallée, and C. Flytzanis, *ibid.* **81**, 922 (1998).

[6] S.G. Han, Z.V. Vardeny, K.S. Wong, O.G. Symko, and G. Koren, Phys. Rev. Lett. **65**, 2708 (1990); G.L. Eesley, J. Heremans, M.S. Meyer, and G.L. Doll, *ibid.* **65**, 3445 (1990).

[7] J. Hohlfeld, J.G. Müller, S.-S. Wellershoff, and E. Matthias, Appl. Phys. B: Photophys. Laser Chem. **64**, 387 (1997).

[8] S.D. Brorson, J.G. Fujimoto, and E.P. Ippen, Phys. Rev. Lett. **59**, 1962 (1987); C. Suárez, W.E. Bron, and T. Juhasz, *ibid.* **75**, 4536 (1995); T. Juhasz, H.E. Elsayed-Ali, G.O. Smith, C. Suarez, and W.E. Bron, Phys. Rev. B **48**, 15 488 (1993).

[9] C.-K. Sun, F. Vallee, L. Acioli, E.P. Ippen, and J.G. Fujimoto, Phys. Rev. B **48**, 12 365 (1993).

[10] W.S. Fann, R. Storz, H.W.K. Tom, and J. Bokor, Phys. Rev. Lett. **68**, 2834 (1992).

[11] R.H.M. Groeneveld, R. Sprik, and A. Lagendijk, Phys. Rev. B **51**, 11 433 (1995).

[12] S.D. Brorson, A. Kazeroonian, J.S. Moodera, D.W. Face, T.K. Cheng, E.P. Ippen, M.S. Dresselhaus, and G. Dresselhaus, Phys. Rev. Lett. **64**, 2172 (1990).

[13] P.B. Allen, Phys. Rev. Lett. **59**, 1460 (1987).

[14] *Handbook of Optical Constants of Solids I/II*, edited by D. Palik (Academic Press, London, 1985/1991).

[15] J.P. Girardeau-Montaut and C. Girardeau-Montaut, Phys. Rev. B **51**, 13 560 (1995).

[16] J. Hohlfeld, S.-S. Wellershoff, J. Güdde, U. Conrad, V. Jähnke, and E. Matthias, Chem. Phys. (to be published).

[17] S.I. Anisimov, B.L. Kapeliovich, and T.L. Perel'man, Zh. Éksp. Teor. Fiz. **66**, 776 (1974) [Sov. Phys. JETP **39**, 375 (1974)]; S.I. Anisimov, and B. Rethfeld, Proc. SPIE **3093**, 192 (1997).

[18] C. Kittel, *Introduction to Solid State Physics* (Wiley, New York, 1996).

[19] J. Hohlfeld, Ph.D. thesis, Freie Universität, Berlin, 1998.

[20] A.P. Kanavin, I.V. Smetanin, V.A. Isakov, Y.V. Afanasiev, B.N. Chichkov, B. Wellegehausen, S. Nolte, C. Momma, and A. Tünnermann, Phys. Rev. B **57**, 14 698 (1998).

[21] W.H. Press, S.A. Teukolsky, W.T. Vetterling, and B.P. Flannery, *Numerical Recipes in C* (Cambridge University Press, Cambridge, 1994).

[22] H.E. Elsayed-Ali, P.B. Corkum, E. Brunel, N.K. Sherman, and T. Srinivasan-Rao, Phys. Rev. Lett. **64**, 1846 (1990).

[23] Calculated according to Allen (Ref. 13) with $\lambda = 0.38$ [W.L. McMillan, Phys. Rev. **167**, 331 (1968)] and estimated $\langle \omega^2 \rangle \sim 722$ meV^2 [J. Braun, K.L. Kostov, G. Witte, L. Surnev, J.G. Skofronick, S.A. Safron, and C. Wöll, Surf. Sci. **372**, 132 (1991)]. Slightly different values were reported by Sanborn, Allen, and Papaconstantopoulos (Ref. 24).

[24] B.A. Sanborn, P.B. Allen, and D.A. Papaconstantopoulos, Phys. Rev. B **40**, 6037 (1989).

[25] F. Budde, T.F. Heinz, M.M.T. Loy, J.A. Misewich, F. de Rougemont, and H. Zacharias, Phys. Rev. Lett. **66**, 3024 (1991).

[26] L.M. Struck, L.J. Richter, S.A. Buntin, R.R. Cavanagh, and J.C. Stephenson, Phys. Rev. Lett. **77**, 4576 (1996).

[27] M. Bonn, S. Funk, Ch. Hess, D.N. Denzler, C. Stampfl, M. Scheffler, M. Wolf, and G. Ertl, Science **285**, 1042 (1999).

[28] F. Budde, T.F. Heinz, M.M.T. Loy, and J.A. Misewich, Surf. Sci. **283**, 143 (1993).

[29] T.A. Germer, J.C. Stephenson, E.J. Heilweil, and R.R. Cavanagh, J. Chem. Phys. **101**, 1704 (1994).

[30] H. Behrens and G. Ebel, Phys. Daten **18-1**, 153 (1981).